sciendo
ISSN 1335-8871
MEASUREMENT SCIENCE REVIEW
Journal homepage: https://content.sciendo.com

Influence of the Electrical Test Setup on the Voltage Gain Measurement of an Unloaded Rosen-Type Piezoelectric Transformer Vibrating in the First Three Modes

Faiza Boukazouha[1*], Hamza Barkat[2], Abdesselam Rouabha[2], Abderahim Herbadji[2], Mohamed Rguiti[3]

[1]*Research Center in Industrial Technologies, CRTI, EChahid Mohammed ABASSI, Algiers, Algeria, faiza_bouka@yahoo.fr, f.boukazouha@crti.dz*
[2]*Calibration, analysis, measurement workshop, Research Center in Industrial Technologies, CRTI, EChahid Mohammed ABASSI, Algiers, Algeria, cndlab@crti.dz*
[3]*Université Polytechnique Hauts-de-France, INSA Hauts-de-France, CERAMATHS – Laboratoire de Matériaux Céramiques et de Mathématiques, F-59313 Valenciennes, France, mohamed.rguiti@uphf.fr*

Abstract: In recent years, Piezoelectric Transformers (PTs) have become a great success due to their excellent properties, especially in applications requiring high voltage. The Rosen-type PT is well known for this performance, as its voltage gain at the resonant frequency can reach few thousands. However, the high output impedance of this device can make an accurate electrical measurement of the output voltage difficult, hence the need to ensure good impedance matching along the measuring electrical test setup. For this purpose, two high impedance oscilloscope probes were successively added to the secondary side to further emulate the measurement chain and match the experiments as closely as possible with the developed 1D model. Accordingly, for an unloaded Rosen type piezoelectric transformer, made of hard ceramic (pz26) with corresponding dimensions 2L×w×t =25 mm×3 mm×2 mm and operating in the first three modes, the corresponding input impedances Z_{in} were evaluated at 665 Ω - 225 Ω and 1974 Ω, while the output impedances Z_{out} were evaluated at 19.2 MΩ - 15.4 MΩ, and 1.8 MΩ. A voltage gain of 164, 179 and 23 at frequencies of 69.4 kHz, 136 kHz and 204.6 kHz, respectively was successfully measured, with a precision of less than 5%. In addition, a detailed equivalent circuit of the transformer was built and all its lumped RLC components were experimentally identified using the Nyquist diagram showing, on the whole, a well-accepted agreement with the expected results.

Keywords: Piezoelectricity, transformer, input impedance, output impedance, probes, voltage gain.

1. INTRODUCTION

In 1880, the Curie brothers discovered together the direct effect of piezoelectricity. In that same year, Lippmann predicted the inverse effect of piezoelectricity, which was immediately confirmed by Curie. However, it was only during the First World War, i.e. 35 years later, that the first concrete industrial application of piezoelectricity occurred with the construction of the first sonar in 1917, which paved the way for a multitude of applications that made intensive use of this natural phenomenon in the medical, military or aeronautical fields. At the end of the 1950s, Rosen proposed and developed an original new device based on the simultaneous use of both effects of piezoelectricity, known as the Piezoelectric Transformer (PT), whose main function was to convert one electrical voltage into another. This smart invention appeared as an ineluctable alternative to the conventional electromagnetic transformers, which have the disadvantage of being heavy, bulky, and above all, unsafe. In fact, this type of device offers plenty of advantages that make it attractive for a wide range of applications, including power supplies for electronic devices [1]. First, a typical PT is easy to manufacture and use in practical terms. It weighs only a few grams with a reduced volume of a few mm^3. In terms of performance, it operates in a wide frequency range (from a few kHz to a few MHz), delivering voltages of up to a few hundred Volts with power densities and efficiencies of up to 100 W/cm^3 and 95%, respectively [2], [3], [4]. Finally, in terms of safety, economic and environmental aspects, the PT does not contain wires, so there is no risk of flammability. It is also marketed at affordable prices and tends to last for many years. Furthermore, it does not generate electromagnetic noise, operates without heat losses and, fortunately, since the banning of lead from the industrial production of piezoelectric ceramics [5], it is no longer considered toxic, which opens up a bright future for it.

In generally, the PTs, which have in common that they only operate at the resonant frequency, can be divided into the following three main categories based on the countless existing architectures:

DOI: 10.2478/msr-2024-0019
**Corresponding author: faiza_bouka@yahoo.fr (F. Boukazouha)*

- The Rosen-type, the most popular and referenced transformer (k_{31}, k_{33} coupling) [6],
- Those that utilize the thickness vibration mode (k_{33}, k_{33} coupling) [7],
- Those based on the planar or radial mode (k_p or k_t coupling) [8].

This paper covers the Rosen-type and comprises the following parts:

The first part is devoted to the presentation of a one-dimensional analytical model describing the electromechanical behavior of the transformer through an electrical equivalent circuit. On the one hand, the transfer functions are calculated, from which the resonant frequencies, the input and output impedances, and the no-load voltage gain as a function of the frequency as well as the values of the circuit parameters can be theoretically derived. On the other hand, all lumped components of the equivalent circuit are identified experimentally by applying the standard method adopted by the Institute of Electrical and Electronics Engineering (IEEE) [9].

The second part focuses on the experimental measurement of the no-load voltage gain in the most precise way possible. In fact, the open circuit voltage gain of this type of PTs can reach several thousands, so its measurement is highly dependent on the selected measurement chain. It is worth noting that although there is no shortage of models describing PT behavior in the literature, most of them have not been able to accurately match experience with theory as long as the oscilloscope was used as the only measurement instrument to quantify the output voltage. As a result, discrepancies between the measured and calculated voltage gain were unfortunately regularly observed [10], [11], [12]. The main cause of these discrepancies is the high value of the output impedance, specific to the Rosen-type transformer (hundreds of MΩ). Moreover, it has been demonstrated that the voltage gain decreases abruptly when the secondary of the PT is charged [13]. In fact, the input impedance of the oscilloscope (1 MΩ) behaves during the measurement as if it were an electrical load connected to the secondary and obviously distorts the measurement of the "no-load gain" in this case. However, by using an operational amplifier (TL081 NC) to increase the input impedance of the circuit, Cellucci et al. managed to measure an open circuit gain of 453, while the estimated gain was 1100 [14]. Another way to overcome this difficulty is to carefully ensure good impedance matching in the measurement chain. To do this, the input and output impedances of the PT should be measured in advance. Then, two oscilloscope probes (1:10 and 1:100), whose role is to augment the effective impedance of the oscilloscope loading the PT, are successively added to the measurement chain. In this way, we can finally confirm whether the output voltage measurement is closely related to the output impedance. Finally, all the results obtained are analyzed, discussed and compared.

2. ROSEN-TYPE PIEZOELECTRIC TRANSFORMER

The Rosen-type piezoelectric transformer bears the name of its inventor. It was originally built from a monolithic, long bar of barium titanate ($BaTiO_3$), which was later replaced by lead zirconate titanate (PZT), which offers higher electromechanical coupling factors (more than 0.7) and higher mechanical quality factors (more than 1000). In any piezoelectric transformer, it is the choice of the electrode placement that separates the primary and secondary areas. In the Rosen-type, three separate electrodes are arranged on a long thin bar, as shown in Fig. 1. The half left part, which is polarized in its thickness direction, constitutes the primary, while the half right part, which is polarized in its length direction, represents the secondary. This judicious configuration allows to create two different vibration modes within the same bar, making it a step-up voltage transformer ideal for backlighting cold cathode fluorescent lamps. Specifically, when an alternative voltage V_1 is applied between the input electrodes, the entire structure begins to vibrate. Firstly, the transverse mode 31 is generated in the material through the electromechanical coupling factor k_{31} (inverse effect). Secondly, in the secondary part, the longitudinal mode 33 produces an electrical field (direct effect) through the electromechanical coupling factor k_{33}. Consequently, a voltage V_2 is generated between the output electrodes. The voltage gain V_2/V_1 reaches its maximum value when the bar is excited near resonance. In this work, we are interested in the study of the first three modes of vibration. The mechanical displacement distribution as a function of position along the length direction of the bar is shown in Fig. 2 for each mode.

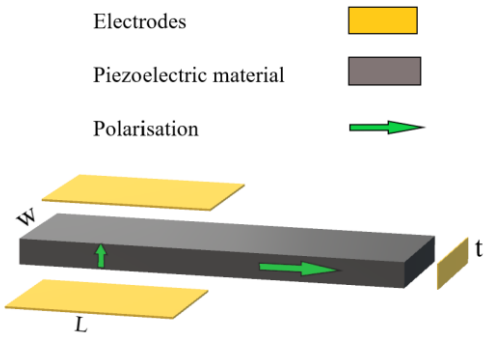

Fig. 1. Position of electrodes, direction of polarizations in a Rosen type PT.

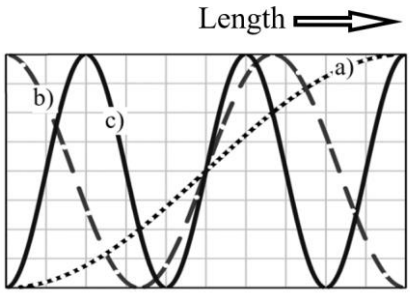

Fig. 2. Displacements profiles of the piezoelectric transformer operating in: a) the fundamental mode $\lambda/2$, b) the second mode λ and c) the third mode $3\lambda/2$.

The Rosen-type PT investigated in this study is made of a lead zirconate titanate (PZT) ceramic supplied by the Danish company Ferroperm. From a large selection of products, our choice went to the pz26 ceramic [15]. The material constants

and dimensions used for modeling were provided by the manufacturer and are listed in Table 1.

Where ρ is the piezoelectric material density. s^E_{11}, s^D_{33} denote the compliance constants along the 13/33 directions, d_{31}, g_{33} denote the piezoelectric constants, ε^T_{33}, β^T_{33} denote the dielectric constants, Q is the mechanical quality factor, $2L$ is the total length, w is the width, and t is the thickness.

Table 1. PZ26 piezoceramic parameters.

Constants	Values
ρ [kg·m^{-3}]	7700
s^E_{11}, s^D_{33} [m^2·N^{-1}]	13×10^{-12}, 11×10^{-12}
$\varepsilon^T_{33}/\varepsilon_0$	1300
d_{31} [m·V^{-1}]	-130×10^{-12}
g_{33} [V·m·N^{-1}]	28×10^{-12}
k_{31}, k_{33}	-0.33, 0.68
Q	1000
$2L\times w\times t$ [mm^3]	25×5×3

A. Mason's 1D model presentation, electrical equivalent circuit

Many analytical and numerical models have been developed to interpret the mechanisms of vibration generation and transfer in PTs [16], [17], [18], [19], [20]. In this work, to predict the electromechanical behavior of the Rosen-type PT, an analytical model taking only a single assumption into consideration is presented: if the thickness and width of the transformer are smaller than its length, only longitudinal waves along the length of the PT (x axis) can be considered. In practice, the primary vibrates in a direction perpendicular to the electric field E (mode 31), while the secondary vibrates in a direction parallel to the electric field E (mode 33). This dynamic system can be modeled using differential equations that govern the wave propagation in solids and equations of motion that include the stress T, the mechanical deformation S, the electric field E and the dielectric displacement D. They can be expressed as [21]:

For the primary side, working as an actuator, two independent variables (T, E) are set:

$$\rho \frac{\partial u_1}{\partial t^2} = \frac{\partial T_1}{\partial x_1} \quad (1)$$

$$S_1 = s^E_{11} T_1 + d_{31} E_3 \quad (2)$$

$$D_3 = \varepsilon^T_{33} E_3 + d_{31} T_1 \quad (3)$$

And for the secondary side, working as a sensor, two independent variables (T, D) are set:

$$\rho \frac{\partial u_3}{\partial t^2} = \frac{\partial T_3}{\partial x_3} \quad (4)$$

$$E_3 = \beta^T_{33} D_3 - g_{33} T_3 \quad (5)$$

$$S_3 = s^D_{33} T_3 + g_{33} D_3 \quad (6)$$

The previous equations can be combined in such a way that both purely electrical and purely mechanical portions can be included, so that an electromechanical behavior becomes clear. The most common and adopted circuits, which are shown in Fig. 3, were developed by Mason as early as 1948 [22]. They are based on the mechanical-electrical analogies, which have one electrical port V, two mechanical ports F, and two mechanical impedances Z_1, Z_2, which depend on the wave velocity, density and frequency. N_1 and N_2 are two ideal electromechanical transformer ratios. C_1 and C_2 represent the static input and output capacitance, respectively.

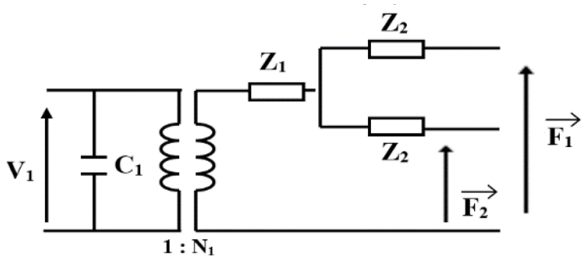

(a) mode 33

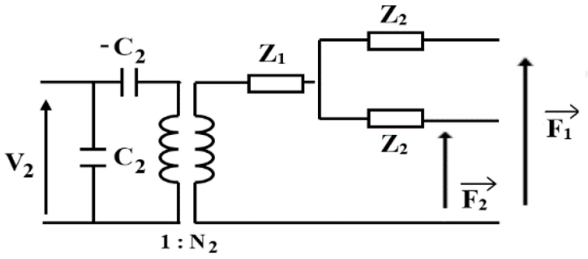

(b) mode 31

Fig. 3. Electromechanical equivalent circuits of both resonators: (a) mode 33, (b) mode 31.

Since the continuity of stress and the mechanical displacement S at the junction and the nullity of stress T at the external free surfaces must be respected, the above circuits are connected in cascade, with the external mechanical ports short-circuited. A global schematization of the equivalent circuit can be obtained after applying several transformations, its final reduced form is shown in Fig. 4. It should be noted that this circuit is only valid around the resonance. It is divided into one RLC resonant branch and two static branches. The inductance L and capacitance C reflect the inertial and potential mechanical energy, respectively, the resistance R takes into account the mechanical losses, while dielectric and piezoelectric losses are ignored. N is the ideal transformation ratio representing the coupling between mechanical and electrical branches. All these lumped components are directly dependent on the PT dimensions, the material properties and additionally on the vibration mode:

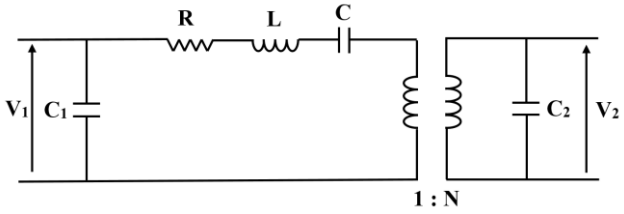

Fig. 4. Lumped parameters model, which describes the behavior of the PT around the resonance.

For the static branches:

$$C_1 = (1-k^2_{31})\, wL/t \quad (7)$$

$$C_2 = (1-k^2_{33})\, wt/L \quad (8)$$

$$N = N_1/N_2 = (d_{31} w\, s_{33}^D)/(C_2\, g_{33}\, s_{11}^E) \quad (9)$$

For the dynamic branch RLC:

$$C = [((\omega_a/\omega_r)^2 -1) \times C_1]/N^2 \quad (10)$$

$$L = 1 / C\omega_r^2 \quad (11)$$

$$R = L\omega_r/Q \quad (12)$$

ω_r and ω_a are the resonance and antiresonance pulsations, respectively.

Finally, the module of the unloaded voltage gain V_2/V_1 at the fundamental mode takes the following symbolic form [23]:

$$|V_2/V_1| = 4/\pi^2 \times k^2 \times Q \times L / t \quad (13)$$

where

$$k^2 = - d_{31}\, g33/s_{11}^E \quad (14)$$

It states that the higher Q and L/t are, the higher the gain.

If you replace the material constants and the transformer dimensions in the above equations with the values listed in Table 1, the value of each component shown in Fig. 4 is determined for the three vibration modes. The values of C_1, C_2, and N remain unchanged regardless of the vibration mode.

However, it should be mentioned that the mechanical loss factor Q is actually lower than the value of 1000 given in the manufacturer's data sheet. First, it was estimated using a piezoelectric disc in planar vibration mode. In addition, the decrease in the quality factor can also be attributed to the clamping of the sample along the vibration direction [24]. Finally, the nature (silver, aluminum, ...), the thickness and the area of the electrodes applied to the material reduce the quality factor to only a few hundred [25], [26], [27]. To get closer to reality, Q is determined experimentally in the next section before it is included in the 1D model.

B. Admittance and impedance measurements, experimental equivalent circuit parameters

Experimentally, it is possible to extract all the values of the lumped components of the equivalent circuit shown in Fig. 4 in order to compare them with the theoretically determined values. This approach, which is based on the analysis of the admittance curves, is often used to characterize piezoelectric resonators in detail [28].

A Hewlett-Packard 4192A LF impedance analyzer generates a sine wave with an amplitude of 1 VRMS to excite the PT. Data is acquired over a frequency range that includes the first three modes in steps of 10 Hz using acquisition software developed in LabVIEW (National Instruments Corp., Austin, TX). The sample is kept free in the air by soldered wires to get as close as possible to ideal conditions (no stress), as shown in Fig. 5.

In the first place, it would be better to determine the experimental value of the mechanical quality factor Q for each mode. For this purpose, the admittance module of the transformer was measured as a function of frequency and plotted in Fig. 6. According to the definition of the Q-factor, it can be expressed as: $Q = f_r /2F$, Q can be measured.

f_r is the resonant frequency, $2F$ is the half-bandwidth (bandwidth at -3 dB).

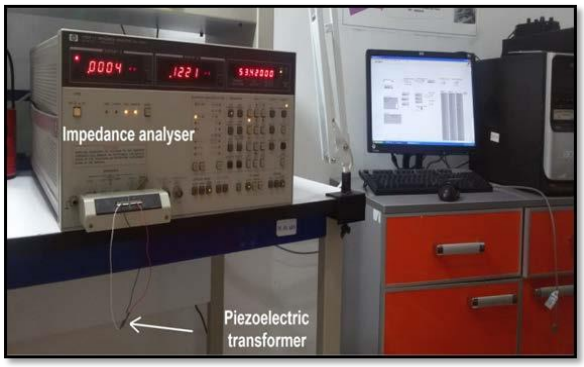

Fig. 5. Experimental bench used for admittance and impedance measurements.

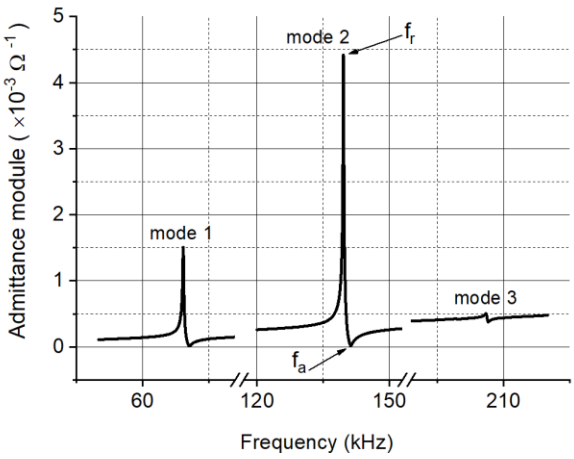

Fig. 6. Variation of the measured input admittance module versus frequency for the first three modes.

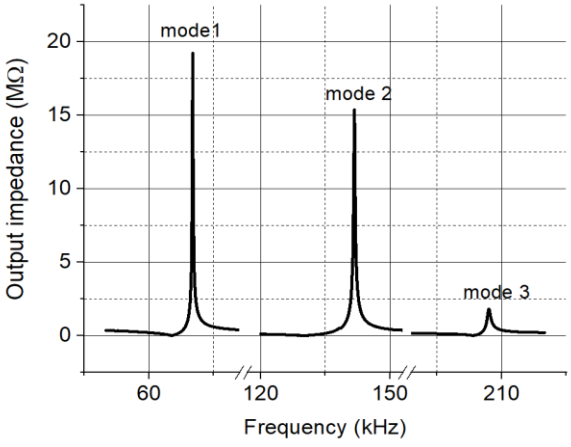

Fig. 7. Variation of the measured output impedance module versus frequency for the first three modes.

The quality factor *Q* of the pz26 ceramic given in Table 1 was about 1000, but the results show that the measured *Q* values of 240, 270, 331 are about 750 lower for the first, second and third mode, respectively. These differences are significant enough that they cannot be neglected. The corresponding input impedances Z_{in} were in the order of a few hundred Ohms (665 Ω, 225 Ω, and 1974 Ω). The measured output impedances Z_{out}, on the other hand, were much larger, evaluated at 19.2 MΩ, 15.4 MΩ and 1.8 MΩ at the first, second and third modes, respectively, as can be seen in Fig. 7. The determination of these values is essential for the rest of the measurements. The equidistant resonant frequencies were determined at 69.2 kHz, 139 kHz, and 205.9 kHz for the first three modes, respectively.

We then used a graphical tool consisting of plotting the imaginary part of the admittance as a function of its real part for the primary *Yp* side and for the secondary *Ys* side. For the primary side, the process was carried out under the condition that the secondary side was short-circuited and vice versa. This process is repeated for each mode, resulting in the six graphs shown in Fig. 8. These obtained curves with the attraction of nearly perfect circles are known as Nyquist diagrams, from which all circuit components can be extracted directly by following the steps detailed in the standard method for studying resonators proposed by the IEEE.

Table 2 shows a complete comparison between the PT equivalent lumped parameter values, the input and output impedances determined by the model performance properties and those determined by the admittance measurements. Despite small differences, the experimental and calculated results agree quite well, especially for the third mode where the relative error is less than 10% for *R*, *L*, *C*, *N*, C_1, and C_2. Based on these experimental values, a novel transfer function is calculated, while the voltage gain and the resonant frequency are determined again.

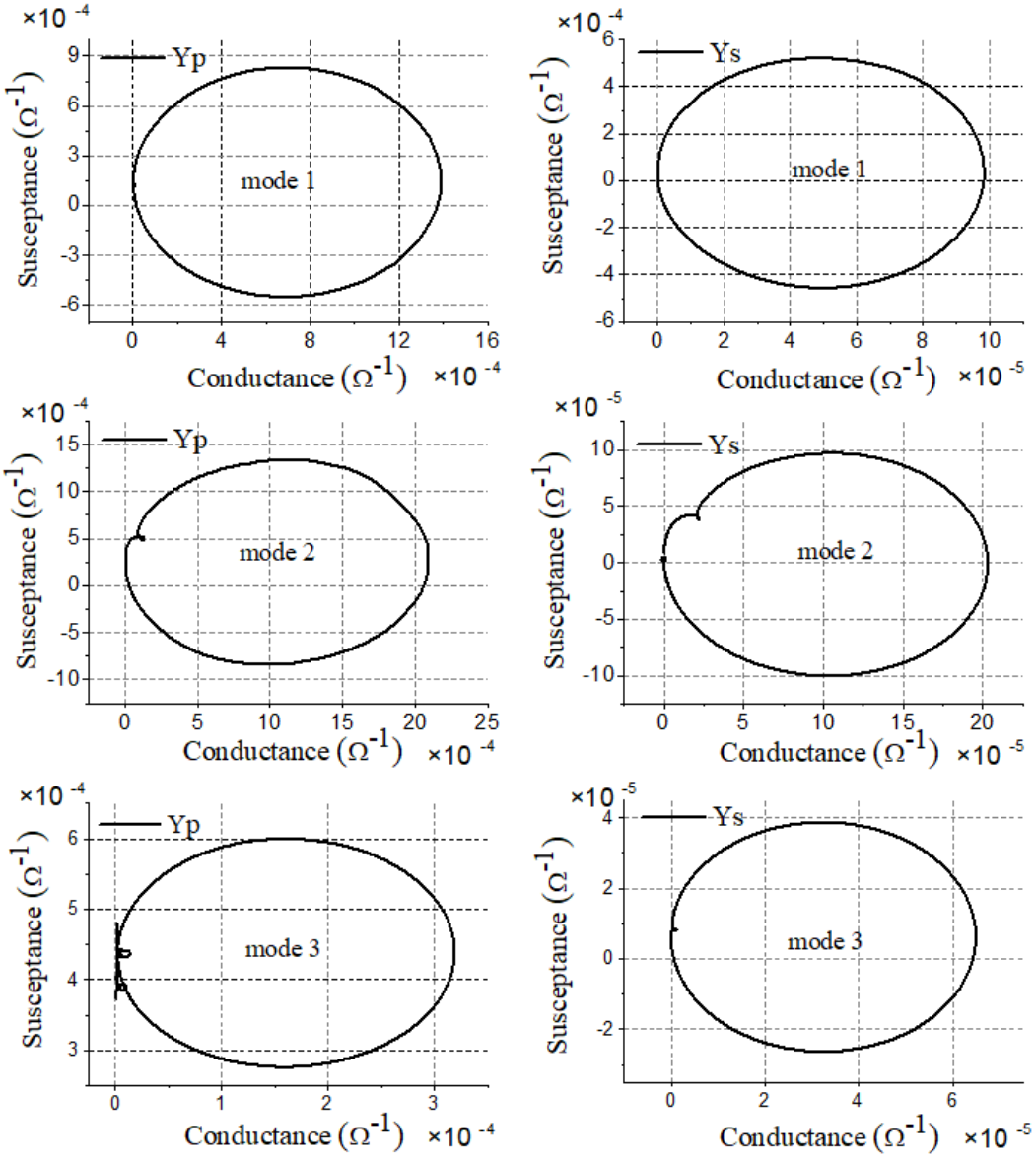

Fig. 8. Admittance circles of the primary and secondary at the first three modes of vibration of the PT.

Table 2. Comparison between the PT equivalent lumped parameters obtained using the 1D model and those identified by the Nyquist diagram.

	mode 1		mode 1		mode 1	
	1D model	measure	1D model	measure	1D model	measure
R [Ω]	9170	10175	4630	4950	19614	19350
C [10-13 F]	11.00	9.94	9.50	9.08	1.66	1.53
L [H]	5.33	5.97	1.52	1.64	3.90	3.99
N	3.96	3.76	3.96	3.21	3.96	3.21
C_1 [10 -10 F]	3.20	3.62	3.20	3.05	3.20	3.20
C_2 [10 -12 F]	4.94	5.33	4.94	4.71	4.94	4.97
Input impedance Z_{in} [Ω]	530	665	282	225	1650	1974
Output impedance Z_{out} [MΩ]	18.70	19.20	13.00	15.40	1.84	1.80

3. UNLOADED VOLTAGE GAIN MEASUREMENT

In this section, the transformer was tested using the test setup shown in Fig. 9. The transformer was driven by an Alternating Current (AC) voltage generated by a function generator HP3314A. A digital oscilloscope LeCroy 64Xi-A was used for the measurement of the input and output voltages. Since the input and output impedances of the transformer must be taken into account, it was necessary to ensure a good impedance adaptation between the generator and the primary side and then between the secondary side and the oscilloscope. If the variable impedance from 10 Ω to 10 kΩ of the function generator can be accurately matched to the input impedance of the transformer, it seems difficult to meet the ideal open circuit condition on the secondary side because the output impedances of the transformer (several tens of MΩ) are still too high compared to the input impedance of the oscilloscope 1 MΩ.

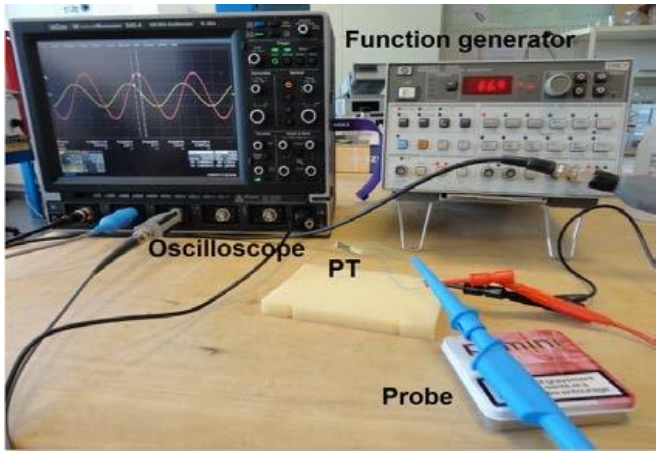

Fig. 9 Input and output voltage measurements.

To increase the effective impedance of the oscilloscope connected to the output of the transformer, a 1:10 probe with an impedance of 10 MΩ was installed in the circuit setup and then replaced by a 1:100 probe Tektronix P5122 with an impedance of 100 MΩ. Only in this way was it possible to obtain a conclusive result, as can be seen in Fig. 10 as an example of the third mode, which shows the variation of the voltage gain as a function of frequency. Using an oscilloscope, it can be seen that the resonance peak occurs at a frequency 200.8 kHz that is more or less close to the expected value 206 8 kHz, but the voltage gain stagnates at 1.9, which is too far from the theoretical value 22.2. Below is a comparison table (Table 3) between the PT voltage gains and the resonant frequencies at the three modes obtained by the 1D model, the experimental Nyquist diagram and various measurements.

It can be noted that the resonant frequency seems to be less affected by the measuring tool than the voltage gain. It can also be observed that the smaller Zout is, the more satisfactory the results are. Overall, the relative error does not exceed 5% for the voltage gain when using a 1:100 probe, while it varies between 50% and 60% when using a 1:10 probe and reaches 90% when using the oscilloscope.

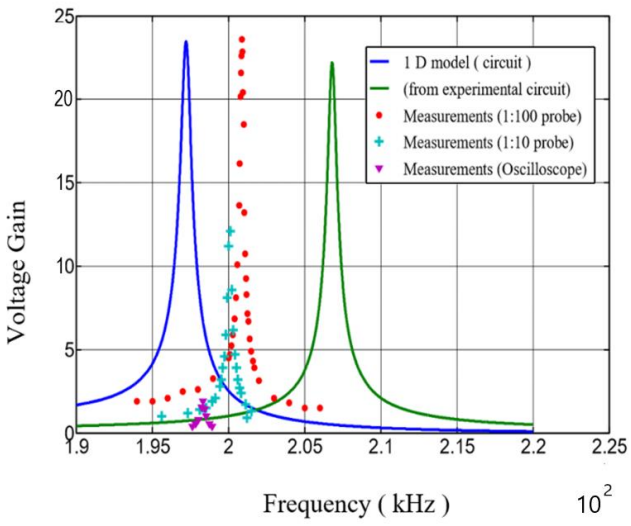

Fig. 10. Variation of the voltage gain as function of frequency at the third mode.

Table 3. Comparison between PT voltage gain and resonance frequency obtained through 1D model, experiment Nyquist diagram and different measurements (oscilloscope, 1:10 probe, 1:100 probe).

Mode		1D model	By Nyquist diagram	Oscilloscope	1:10 probe	1:100 probe
1	Resonance frequency [kHz]	65.7	69.2	65.6	67.1	69.4
	Voltage gain	183	155	5	75	164
2	Resonance frequency [kHz]	138	139.5	130.6	133.7	136.1
	Voltage gain	180	171	17.6	67	179
3	Resonance frequency [kHz]	197.2	206.8	200.8	201.6	204.6
	Voltage gain	23.4	22.2	1.9	12.1	23.6

4. CONCLUSION

Piezoelectric transformers differ from their normal electromagnetic counterparts in one major advantage: the possibility of miniaturization. Over the years, they have gained a good reputation among low-power electronic devices, and their application fields are constantly expanding, promising them a successful future.

In this article, the basic properties of a Rosen-type piezoelectric transformer were analyzed, namely the output impedance and the voltage gain. The experiments were carried out with the aim of measuring the voltage gain of the unloaded PT as accurately as possible for the first three modes of vibration. For this purpose, strict control of the impedance adaptation along the electrical test setup (generator, primary, secondary, and oscilloscope) was required, taking into account the high output impedance of the PT. For this reason, two impedance probes were introduced to further emulate the electrical test setup and to faithfully compare the experiments with the presented 1D model. In addition, a detailed equivalent circuit analysis of the transformer was performed, and the results were in good agreement with the experimental results.

REFERENCES

[1] Carazo, A. V. (2016). Piezoelectric transformers: An historical review. *Actuators*, 5 (2), 12. https://doi.org/10.3390/act5020012

[2] Du, J., Hu, J., Tseng, K.-J. (2004). High-power, multioutput piezoelectric transformers operating at the thickness-shear vibration mode. *IEEE Transactions on Ultrasonics, Ferroelectrics, and Frequency Control*, 51 (5), 502-509. https://doi.org/10.1109/TUFFC.2004.1320823

[3] Vangordon, J. A., Gall, B. B., Kovaleski, S. D., Baxter, E. A., Almeida, R., Kwon, J. W. (2010). High voltage production from shaped piezoelectric transformers and piezoelectric transformer based circuits. In *2010 IEEE International Power Modulator and High Voltage Conference*. IEEE, 334-337. https://doi.org/10.1109/IPMHVC.2010.5958361

[4] Seo, J. M., Choi, J. H., Moon, C. W., Sung, H. G. (2005). Optimal design of piezoelectric transformer for high efficiency and high power density. In *2005 International Conference on Electrical Machines and Systems*. IEEE, 2290-2295. https://doi.org/10.1109/ICEMS.2005.202978

[5] Commission of the European Communities. (2008). *Proposal for a directive of the European parliament and of the council on the restriction of the use of certain hazardous substances in electrical and electronic equipment*. Document 52008PC080. https://eur-lex.europa.eu/legal-content/EN/TXT/?uri=celex%3A52008PC0809

[6] Rosen, C. A. (1956). Ceramic transformers and filters. In *Proceedings of the 7th Electronic Components Symposium*. New York, US: Engineering Publishers, 205-211.

[7] Ohnishi, O., Kishie, H., Iwamoto, A., Sasaki, Y., Zaitsu, T., Inoue, T. (1992). Piezoelectric ceramic transformer operating in thickness extensional vibration mode for power supply. In *IEEE 1992 Ultrasonic Symposium Proceedings*. IEEE, 483-488. https://doi.org/10.1109/ULTSYM.1992.275961

[8] Baker, E. M., Huang, W., Chen, D. Y., Lee, F. C. (2005). Radial mode piezoelectric transformer design for fluorescent lamp ballast applications. *IEEE Transactions on Power Electronics*, 20 (5), 1213-1220. http://dx.doi.org/10.1109/TPEL.2005.854068

[9] IEEE. (1966). *177-1966 - IEEE Standard Definitions and Methods of Measurement for Piezoelectric Vibrators*. https://doi.org/10.1109/IEEESTD.1966.120168

[10] Jung, S.-Y. , Lee, G., Kim, T.-W., Kim, S. J., Koh, J. H. (2023). Rosen-type piezoelectric transformers based on $0.5Ba(Zr_{0.2}Ti_{0.8})O_3–0.5(Ba_{0.7}Ca_{0.3})TiO_3$ ceramic and doped with Sb_2O_3. *Materials*, 16 *(*18), 6201. https://doi.org/10.3390/ma16186201

[11] Hwang, L., Yoo, J., Jang, E., Oh, D., Jeong, Y., Ahn, I., Cho, M. (2004). Fabrication and characteristics of PDA LCD backlight driving circuits using piezoelectric transformer. *Sensors and Actuators*, A 115, 73-78. http://dx.doi.org/10.1016/j.mseb.2007.01.031

[12] Hsu, Y.-H., Lee, C.-K., Hsiao, W.-H. (2005). Electrical and mechanical fully coupled theory and experimental verification of Rosen-type piezoelectric transformers. *IEEE Transactions on Ultrasonics, Ferroelectrics, and Frequency Control*, 52 (10), 1829-1839. https://doi.org/10.1109/TUFFC.2005.1561639

[13] Falimiaramanana, D. J., Ratolojanahary, F. E., Lefebvre, J.-E., Maimouni, L. E., Rguiti, M. (2020) 2-D modeling of Rosen-type piezoelectric transformer by means of a polynomial approach. *IEEE Transactions on Ultrasonics, Ferroelectrics, and Frequency Control*, 67 (8), 1701-1714. https://doi.org/10.1109/TUFFC.2020.2975647

[14] Cellucci, G., Pirani, S., Galassi, C., Capiani, C., Watts, B. E., Melioli, E., Leccabue, F. (1999). The fabrication and testing of a piezoelectric transformer. *Ferroelectrics,* 228 (1), 129-137. https://doi.org/10.1080/00150199908226131

[15] Meggitt Ltd. *Ferroperm Piezoceramics product line*. http://meggittsensingsystems.com/

[16] Syed, E. M. (2001). *Analysis and modeling of piezoelectric transformers.* Thesis, University of Toronto, Canada. https://tspace.library.utoronto.ca/handle/1807/16429

[17] Joo, H., Kim, I., Song, J., Jeong, S., Kim., M. (2010). Piezoelectric properties of Rosen-type piezoelectric transformer using 0.01Pb ($Ni_{1/3}Nb_{2/3}$) O_3 - 0.08Pb ($Mn_{1/3}Nb_{2/3}$) O_3-0.91Pb ($Zr_{0.505}Ti_{0.495}$) O_3. *Journal of the Korean Physical Society*, 56 (1), 374-377. http://dx.doi.org/10.3938/jkps.56.374

[18] Nadal, C. (2012). *Contribution à la conception et la modélisation de transformateurs piézoélectriques dédiés à la génération de plasma*. Thesis, Institut National Polytechnique de Toulouse, France. https://theses.hal.science/file/index/docid/639894/filename/nadal.pdf

[19] Chang, K. T. (2005). Transient response analysis of a Rosen-type piezoelectric transformer and its applications. *IEEE Trans Ultrasonics, Ferroelectrics, and Frequency Control*, 52 (9), 1534-1545. https://doi.org/10.1109/tuffc.2005.1516026

[20] Fernandez, J. M., Holzbecher, J., Stutz, M., Perriard, Y. (2005). Modeling and characteristics comparison of two different piezoelectric transformers. In *IEEE Ultrasonics Symposium*. IEEE, 1530-1533. https://doi.org/10.1109/ULTSYM.2005.1603150

[21] IEEE. (1988). *176-1987- IEEE Standard on Piezoelectricity*. https://doi.org/10.1109/IEEESTD.1988.79638

[22] Mason, W. P. (1948). *Electromechanical Transducers and Wave Filters. Second Edition.* D. Van Nostrand Company, Inc., ISBN 978-0442051648.

[23] Mezheritsky, A. (2006). Quality factor concept in piezoceramic transformer performance description. *IEEE Transactions on Ultrasonics, Ferroelectrics, and Frequency Control*, 53 (2), 429-420. http://dx.doi.org/10.1109/TUFFC.2006.1593382

[24] Rajapurkar, A. M. (2008). *Loss mechanisms in piezoelectric PZT ceramics and single crystals.* Thesis, Pennsylvania State University, US. https://etda.libraries.psu.edu/catalog/8809

[25] Du, J., Hu, J., Tseng, K. J. (2004). High-power, multioutput piezoelectric transformers operating at the thickness-shear vibration mode. *IEEE Transactions on Ultrasonics, Ferroelectrics, and Frequency Control*, 51(5), 502-509. http://dx.doi.org/10.1109/TUFFC.2004.1320823

[26] Wei, Z., Hu, J., Li, Y., Chen, J. (2022). Effect of electrode thickness on quality factor of ring Electrode QCM sensor. *Sensors*, 22 (14), 5159. https://doi.org/10.3390/s22145159

[27] Benewell, A. L. (2009). *A high voltage piezoelectric transformer for active interrogation*. Thesis, University of Missouri, Columbia, US. https://doi.org/10.32469/10355/6847

[28] Lin, R.-L. (2001). *Piezoelectric transformer characterization and application of electronic ballast*. Thesis, Virginia Polytechnic Institute and State University, Blacksburg, US. https://vtechworks.lib.vt.edu/items/9fb153b8-e95f-4c27-bfd4-40c641d70c1a

Received January 09, 2024
Accepted July 09, 2024